Impact of Post-Weld Heat Treatment on the Microstructural and Mechanical Behavior of API X70 Steel

Aboubaker Haissam[1], Mohmmed Elhadi Benhorma[2], Souad Benarrache[2,3], H.Aissa Benhorma[2], Kouider Rahmani[4]

[1]*Laboratory of Development in Mechanics and Materials (LDMM), Ziane Achour University of Djelfa, 17000, Algeria*
[2]*Mechanical Laboratory, Amar Telidji University of Laghouat, B.P. 37G Road to Ghardaia 03000 Laghouat, Algeria*
[3]*ENS Laboratory, Ecole Normal Supérieure of Laghouat, Laghouat 03000, Algeria*
[4]*Modelling, Simulation and Optimization of Real Complex Systems Research Laboratory, Ziane Achour University of Djelfa, 17000, Algeria*
Email: as.haissam@univ-djelfa.dz,

Abstract: The global advancement in scientific research within the petroleum sector, particularly in transportation methods, has driven interest in understanding the welding characteristics of petroleum pipelines. This study provides an experimental evaluation of the effects of heat treatments on the mechanical and microstructural properties of welded API X70 steel. Specifically, it investigates the influence of varying heat treatment conditions on the fusion zone (FZ) of API X70 steel welds. The heat treatment process was carried out at temperatures ranging from 450°C to 650°C, in increments of 50°C, with each temperature maintained isothermally for 2 hours. Comprehensive characterization techniques, including optical microscopy, scanning electron microscopy (SEM), and X-ray diffraction (XRD), were employed to analyze the microstructural evolution. Additionally, Vickers hardness testing was conducted to evaluate the mechanical response. The results demonstrated that increasing the heat treatment temperature promoted grain coarsening and growth within the fusion zone, accompanied by a progressive decline in the hardness of the weld joints. These findings highlight the critical role of heat treatment parameters in tailoring the performance of welded pipelines.

Keywords: A X70 API, weld joints, heat treatments, fusion zone FZ, grain growth, scanning electron microscope (SEM), XRD diffraction, hardness

1. Introduction

The industrial domain of hydrocarbons and transport has witnessed significant advancements, largely driven by the enhanced understanding and control of the mechanical and structural properties of High Strength Low Alloy (HSLA) steels. Among these, API X70 steel stands out due to its exceptional mechanical strength, resistance to corrosion, and ability to perform under high-stress and severe environmental conditions. The influence of temperature and holding time on the structural evolution of X70 steel is critical, as these parameters directly affect its mechanical behavior, particularly its tensile strength and resistance to failure under extreme stresses.

In the context of metallurgy, carbon plays a pivotal role in determining the properties of steel. Carbon atoms integrate into the interstitial spaces of the face-centered cubic (FCC) iron lattice, forming a solid solution known as austenite (γ-iron) at elevated temperatures. Conversely, in body-centered cubic (BCC) α-iron, carbon solubility is minimal, forming ferrite. During cooling, carbon's reduced solubility leads to its precipitation as iron carbide (Fe_3C), or cementite, significantly enhancing the alloy's hardness. This

precipitation behavior is governed by the iron-carbon phase diagram, highlighting key transformations, such as the eutectoid reaction at 727°C and 0.77% carbon content [1, 2].

The welding of API X70 steel is vital in the pipeline industry, where it is extensively utilized for transporting high-pressure fluids in oil and gas applications. The welding process introduces complex thermal cycles, resulting in distinct zones, such as the fusion zone (FZ) and the heat-affected zone (HAZ), which undergo microstructural transformations. These transformations alter the mechanical properties, such as toughness, ductility, and hardness, influencing the performance and reliability of welded joints under operational conditions. Welding involves intricate physicochemical phenomena, requiring external energy sources such as electrical, chemical, mechanical (friction), or optical (laser) to facilitate the formation of atomic bonds [3].

Heat treatment is a critical post-welding process that induces microstructural changes, significantly impacting mechanical properties like strength, hardness, and fracture toughness. Understanding these transformations is essential for predicting the long-term behavior of welds and optimizing welding parameters to minimize defects, such as porosity and cracking. Studies indicate that thermal cycles and cooling rates during welding heavily influence the microstructural evolution, necessitating detailed research to develop predictive models and improve manufacturing practices for pipeline systems [4-7].

The role of alloying elements like niobium, aluminum, titanium, and chromium is central to the microstructural refinement and mechanical enhancement of HSLA steels. Niobium and aluminum contribute to grain refinement, with critical particle sizes around 300 Å [8-11]. Titanium forms stable precipitates such as TiN and TiC, which control grain growth, while chromium enhances hardenability, abrasion resistance, and corrosion resistance, particularly in seawater environments when combined with elements like copper and phosphorus [12-14].

A comprehensive analysis was conducted at various temperatures with a constant holding time to study the microstructural development and associated mechanical properties of API X70 welds. The primary focus was on characterizing the structural evolution in the weld bead (fusion zone) and understanding the interplay between metallurgical phases, grain refinement, and precipitation phenomena to achieve optimal weld performance [15-17]. This study contributes to expanding the broader understanding of High Strength Low Alloy (HSLA) steels and their applications in critical industrial sectors.

2. Experimental Methods

The material examined in our study is the weld bead of X70 steel API, measuring 400 mm in length and 15 mm in thickness. The base material and the deposited metal are characterized by their chemical compositions, as presented in Figures 1 and 2 [17,18].

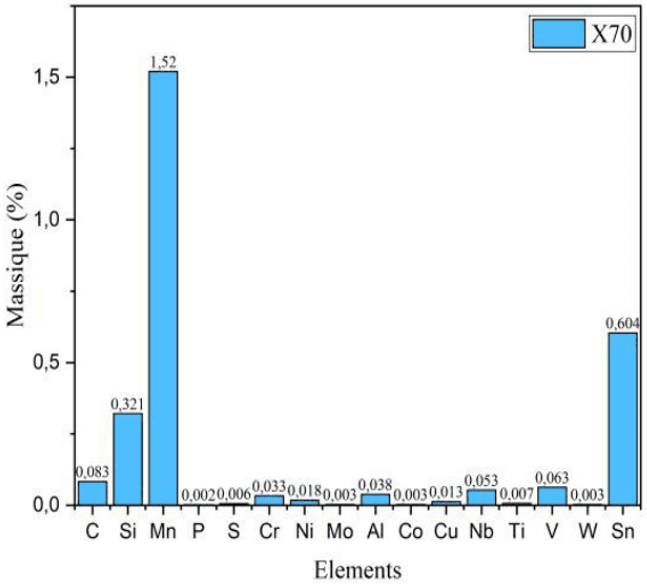

Figure 1. Chemical Composition of X70 Steel API [17].

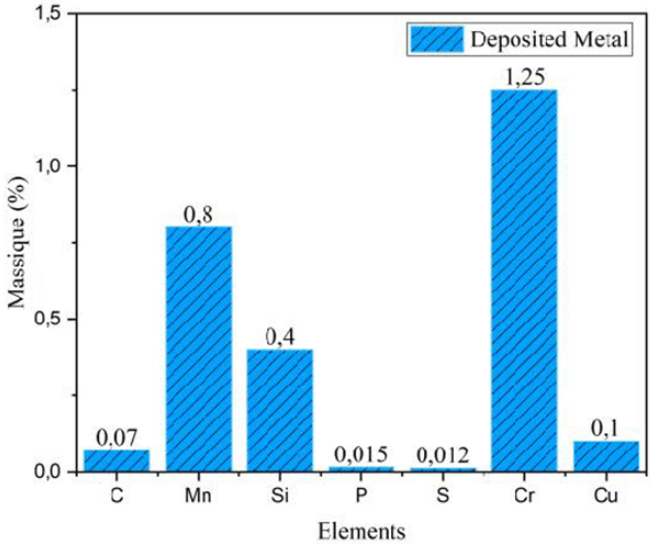

Figure 2. Chemical Composition of deposited metal [17].

The heat treatments in this study were conducted using a NABERTHERM electric furnace, equipped with an insulated chamber measuring 700 × 500 × 250 mm. The furnace utilizes a resistance heater capable of reaching a maximum temperature of 3000 °C. Within the chamber, the temperature is highly uniform, with a gradient of less than 5 °C across different points on the sample [17].

In this study, the heat treatment involved varying the temperature between 450 °C and 650 °C in increments of 50 °C. At each temperature, the samples were held for two hours to ensure thermal stabilization. After heating, the samples were cooled in air at room temperature (25 °C).

To reveal the microstructure after heat treatment, the samples were mechanically polished using silicon carbide abrasive papers of progressively finer grades (80, 400, 600, 800, and 1200 µm). Final polishing was performed using diamond paste with a grain size of 0.25 µm, resulting in a mirror-like surface finish suitable for metallurgical analysis. The samples were then etched with a Nital solution (4% nitric acid and 96% ethanol) for 30 to 60 seconds to reveal their microstructure, removing the mirror finish. Following etching, the samples were rinsed with water to stop the etching process [17].

Microscopic analysis was performed using an optical microscope (LIECA DMLM) equipped with a high-resolution camera. The samples were observed at 1000× magnification, and micrographs were taken at 20 µm magnification. To ensure accuracy, at least five different fields of view were analyzed for each sample. The average grain diameter was determined by counting the grain boundary intersections along a predefined test line superimposed on the micrographs [17].

Vickers hardness testing was performed using a square-based diamond pyramid indenter with a top angle of 136°. The hardness, HV, was calculated using the formula:

$$Hv = 1.8544\, F/\, d^2 \qquad (1)$$

where F is the applied force, and d is the average diagonal length of the indentation. Six measurements were conducted on each sample using a Model MVK-H2 durometer under a load of 300 g. These measurements were performed on the same samples subjected to metallographic analysis.

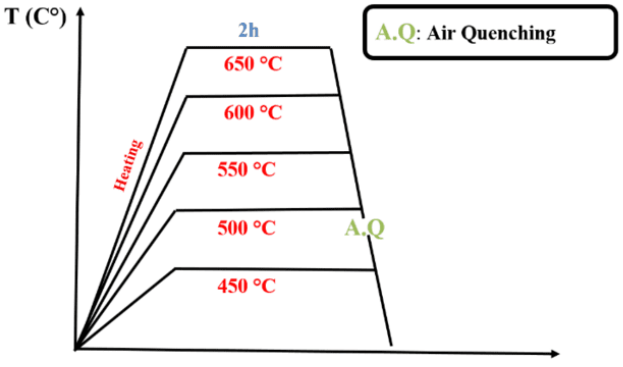

Figure 3. Heat treatment

For X-ray diffraction (XRD) analysis, a Panalytical Empyrean diffractometer was used. X-rays were generated using a Cu anode kα=1,54060A°. Operating parameters for all samples were set at 1 kV and 1 mA, with a step size of 0.0260° and a dwell time of 116.79 seconds per step. Scanning was conducted over a 2θ of (20° -120°), with a total scan time of 30 minutes for each sample.

3. Results and Discussion

3.1 Effect of Heat Treatment on microstructures

Figure 4 presents a micrograph of the fusion zone at different temperatures over a period of 2 hours. The microstructure of the fusion zone (FZ) in welded API X70 steel exhibited distinct changes after exposure to different temperatures.

At 450°C, the microstructure consists of an equiaxed ferritic and pearlitic matrix. At 500°C, the grain size of ferrite and pearlite increases, and the formation of carbides is observed. As the temperature rises to 550°C, the grain size further increases [17], and precipitates of chromium carbide and nickel carbide begin to form (figure 4.c) [19].

This increase is always explained by the gain in energy (heat input), which continuously drives the system (the matrix, alloying elements, and various phases) towards a stable thermodynamic equilibrium. This process is strongly influenced by the alloying elements, the energies of point and line defects (internal stresses), and the interfacial tensions between grains [17,20].

We can illustrate thermodynamic equilibrium using the Gibbs free energy equation:

$$\Delta G = \Delta H - T\Delta S + \sum_i^n Qi \qquad (2)$$

At temperatures T the system is in equilibrium when

$$\frac{\partial G}{\partial T} = 0 \qquad (3)$$

where, ΔG is the change in free energy, ΔH is the change in enthalpy, T is the temperature, ΔS is the change in entropy, and Qi represents the energies of point and linear defects as well as interfacial tensions between grains and dislocations [21].

At 600°C, the formation of chromium carbide, nickel carbide, and molybdenum carbide precipitates is observed (figure 4.d).

At 650°C, the same precipitates as those formed at 600°C are observed, but with a larger grain size (Figure 4.e) [22].

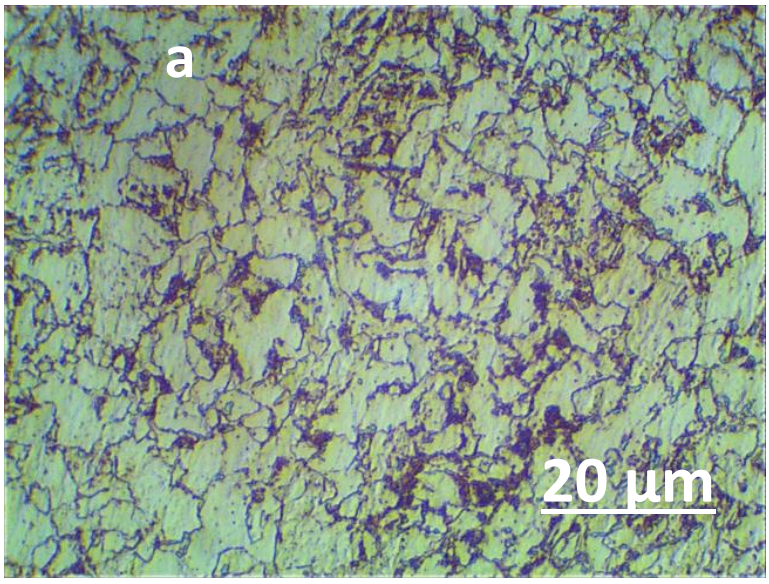

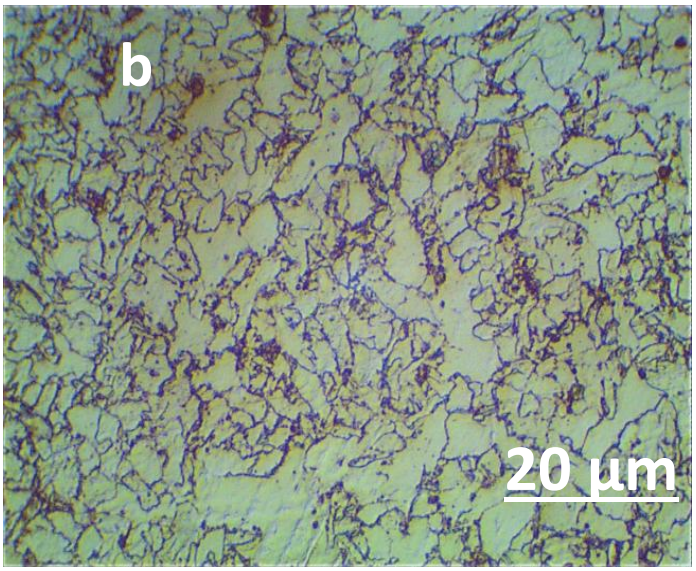
b
20 µm

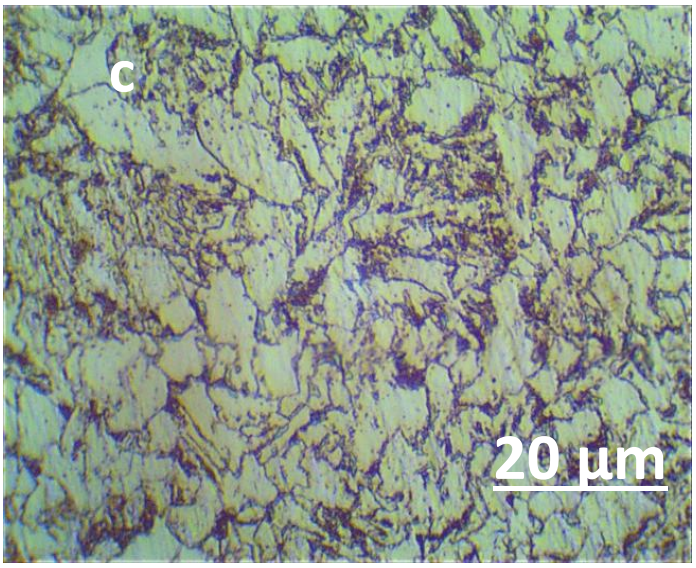
c
20 µm

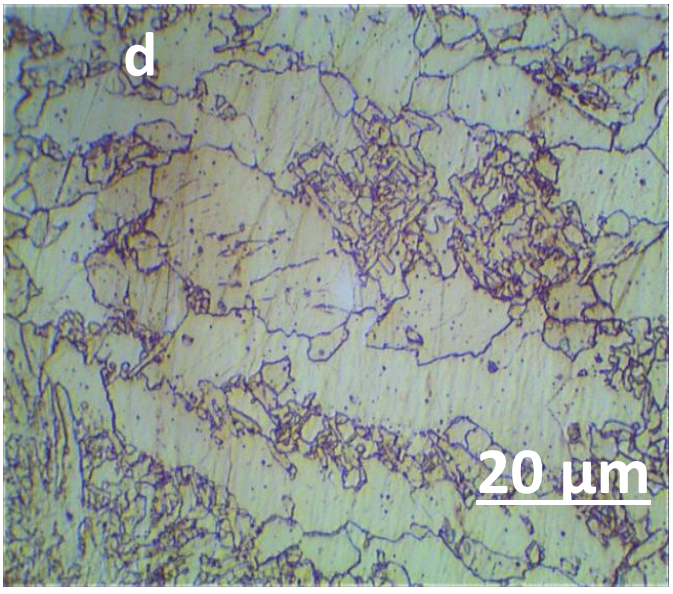
d
20 µm

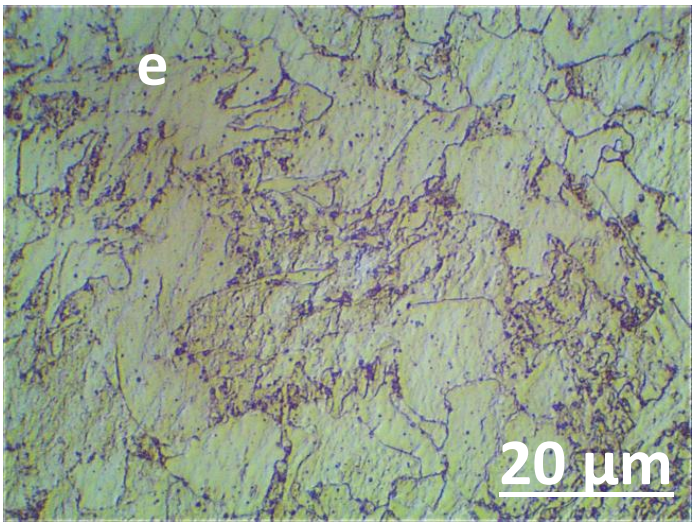

Figure 4: Optical Microstructure of the Weld Bead in X70 Steel After Heat Treatment at Different Temperatures for 2 Hours:
a) 450 °C b) 500 °C c) 550 °C d) 600 °C e) 650 °C

3.2XRD analysis

The X-ray diffraction patterns in Figure 5 show the fusion zone (FZ) of samples subjected to heat treatment. At 650 °C with a holding time of 2 hours, diffraction angles 2θ were observed at (44.5990°), (64.991°), (82.435°), (98.849°), and (116.49°). A noticeable peak shift compared to 450 °C was observed at (44.1429°), (64.410°), (82.248°), (98.777°), and (116.161°). This peak shift, along with variations in the intensity of diffracted peaks, indicates differences in the density of diffracting planes associated with the formation and/or dissolution of various phases, such as chromium and nickel carbides [17].

The X-ray diffraction analysis of API X70 steel samples subjected to heat treatment at different temperatures for a holding time of 2 hours revealed the presence of several coexisting phases: iron matrix (Fe), iron carbide (Fe_3C), chromium carbides ($Cr_{23}C_6$), molybdenum carbides (Mo_2C), vanadium carbide (VC), niobium carbide (NbC), titanium carbide (TiC), and nickel carbide (Ni_3C).

The micrograph (Figure 5) shows a progressive increase in grain size with rising temperature. At 550°C, the diffraction patterns (Figure 5.c) are dominated by the (200) reflection of aluminum nitride (AlN), chromium carbide ($Cr_{23}C_6$), and nickel carbide (Ni_3C), indicating their predominant presence. However, the presence of Fe_3C is also evident through its (102) and (220) reflections.

For temperatures ranging between 600°C and 650°C, the reappearance of $Cr_{23}C_6$, Ni_3C, VC, TiC, WC, and Mo_2C phases becomes significant in the diffraction patterns (Figures 5.c, 5.d, and 5.e), as evidenced by the emergence of their respective (133), (113), and (200) reflections.

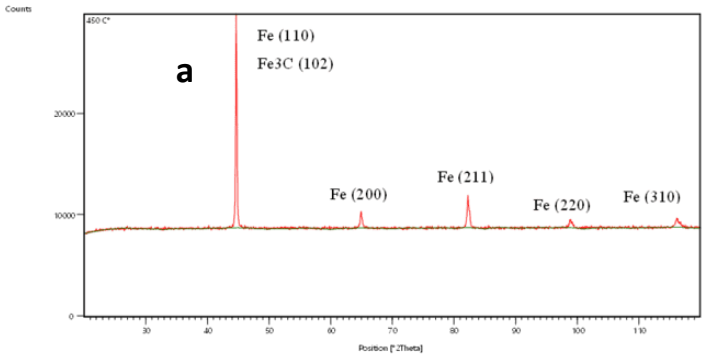

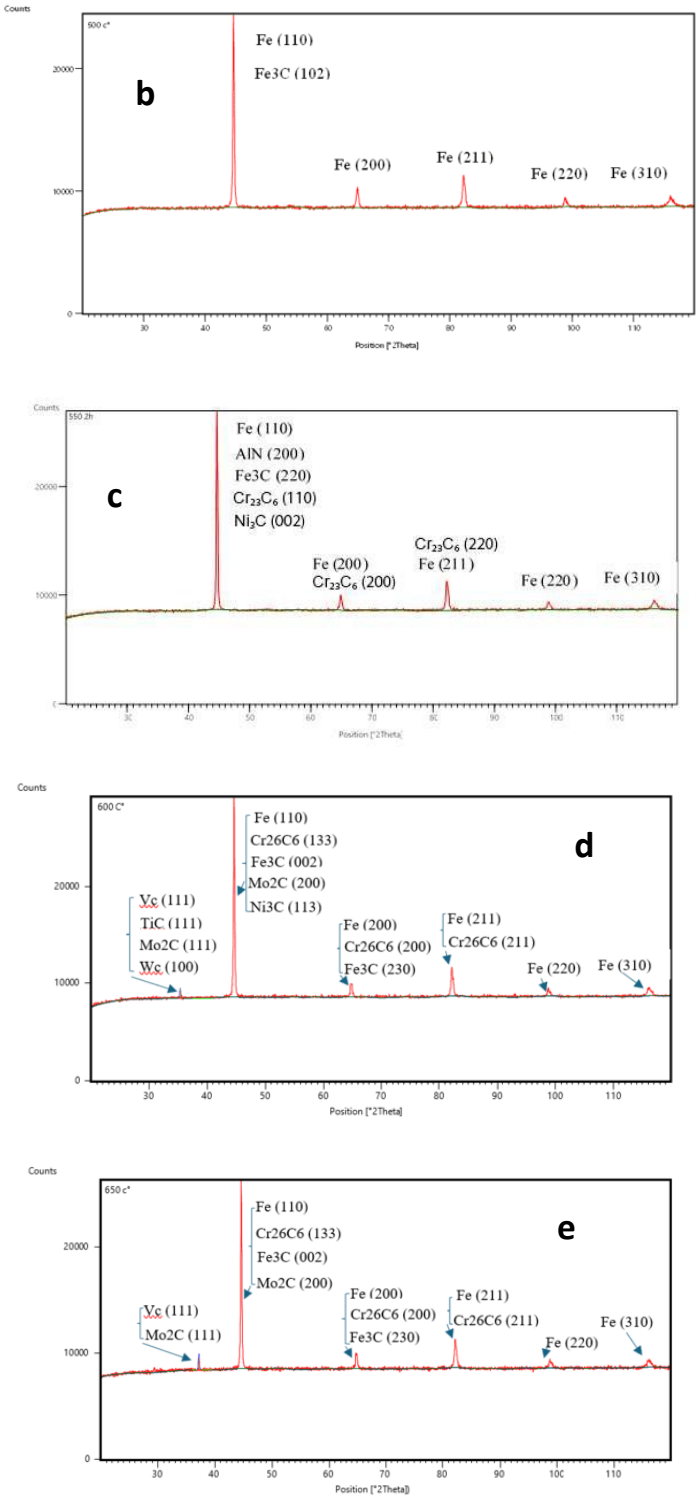

Figure 5: Diffraction Patterns of the Fusion Zone (FZ) of the Weld Bead at Various Temperatures for 2 Hours: a) 450 °C b) 500 °C c) 550 °C d) 600 °C e) 650 °C

3.3 Effect of heat treatment on hardness

Figure 6 shows the hardness (HV) as a function of the different temperatures over a period of 2 hours. It can be observed that with the increase in temperature up to 550°C, the hardness increases from 184 HV to 237 HV. This increase is attributed to the grain size, the dissipation of dislocations (internal stresses), and the formation of chromium carbide ($Cr_{23}C_6$) and nickel carbide (Ni_3C) [23-25].

This can be interpreted using the law of dislocation mobility rate:

$V = \alpha exp\left((-\Delta H_i)/RT\right)$ (4)

where:

- V : Dislocation mobility velocity.
- ΔH_i: Activation enthalpy of a dislocation at temperature T.
- R : Universal gas constant.

In this context, the dissipation velocity of dislocations, initially measured in single-crystal materials such as silicon (Si), is significantly influenced in alloys by the presence of impurities and alloying elements. These elements, whether interstitial or in the form of carbide precipitates, alter the mechanical properties and the mobility of dislocations [17].

This dissipation rate is measured in pure grains (e.g., Si). In our case, this rate will depend heavily on the impurities present within the grains, such as the existence of different alloying elements in the interstitials or carbides within the matrix.

As the temperature increases to 650°C, the hardness decreases from 237 HV to 200 HV. This decrease is due to the replacement of chromium carbide ($Cr_{23}C_6$) and nickel carbide (Ni_3C) by molybdenum carbide (Mo_2C) and vanadium carbide (VC), as well as the increased grain size of the carbides.

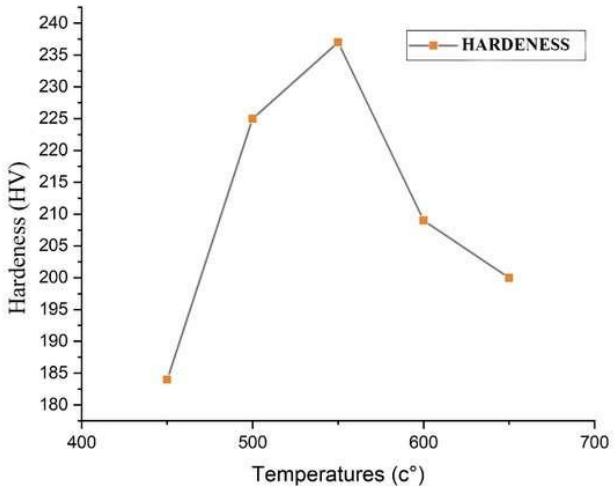

Figure 6 Measurement of microhardness as a function of different heat treatment temperatures for a fixed time of 2 hours.

4. Conclusions

In conclusion, the X-ray diffraction analysis of API X70 steel treated at various temperatures for 2 hours revealed the formation and dissolution of several carbides, including chromium, nickel, molybdenum, and vanadium carbides. As the temperature increased, the grain size grew, and diffraction patterns showed significant changes, indicating phase transformations. At higher temperatures (600°C to 650°C), the presence of additional carbides like Mo_2C and VC became prominent, highlighting the temperature-dependent evolution of the material's microstructure.

1. The microstructure of the fusion zone (FZ) in API X70 steel, analyzed at different temperatures over a period of 2 hours, revealed distinct changes. At lower temperatures (450°C), the microstructure consists of equiaxed ferritic and pearlitic phases. As the temperature increases to 500°C and 550°C, the grain size enlarges, and carbide formation (chromium and nickel carbides) begins. This increase in grain size and carbide formation is attributed to the energy input from heat, driving the system toward a thermodynamic equilibrium, influenced by alloying elements and internal stresses. At higher temperatures (600°C and 650°C), further carbide precipitates, including molybdenum carbide, are formed, with an increase in grain size. These changes can be explained using the Gibbs free energy equation, which considers the contributions of enthalpy, entropy, and defect energies to the system's overall stability. The results highlight the significant impact of temperature on phase formation and microstructure evolution in the welded API X70 steel.
2. The hardness (HV) of API X70 steel, as shown in Figure 6, increases with temperature up to 550°C, rising from 184 HV to 237 HV. This increase in hardness is attributed to several factors, including the grain size, the dissipation of dislocations, and the formation of chromium and nickel carbides. The dislocation mobility rate, which can be expressed using the activation enthalpy and the

presence of alloying elements, influences the hardness, particularly in alloys where impurities and carbide precipitates modify the dislocation movement. However, as the temperature increases further to 650°C, the hardness decreases from 237 HV to 200 HV. This decrease is due to the replacement of chromium and nickel carbides with molybdenum and vanadium carbides, along with an increase in the grain size of the carbides. This behavior highlights the dynamic interplay between temperature, phase transformations, and dislocation mobility in the material.

References

1. Callister, W.D. (2020). Materials Science and Engineering: An Introduction. John wiley & sons.
2. Dupeux, M. (2008). Aide-Mémoire de Science des Matériaux - 2ème Édition. Dunod.
3. Jeffus, L. (2021). Welding: Principles and Applications (9th ed.). Cengage Learning. ISBN 9780357377659. https://www.cengage.uk/c/welding-principles-and-applications-9e-jeffus/9780357377659/?searchIsbn=9780357377659
4. hu Ming, Kehong Wang, Zeng Liu, Wei Wang, Youqi Wang. (2020). Effect of the cooling rate on the microstructure and mechanical properties of high nitrogen stainless steel weld metals[J]. CHINA WELDING, 29(2): 48-52. http://chinawelding.hwi.com.cn/article/doi/10.12073/j.cw.20200221002
5. Shravan C, N. Radhika, N. H. Deepak Kumar & B. Sivasailam. 2023. A review on welding techniques: properties, characterisations and engineering applications. Materials and Processing Technologies , 10 ,1126-1181. https://doi.org/10.1080/2374068X.2023.2186638
6. Gang Chen, Wei Xue, Yuzhen Jia, Shucheng Shen, Guoyue Liu,)2020). Microstructure and mechanical property of WC-10Co/RM80 steel dissimilar resistance spot welding joint, Materials Science and Engineering: A,Volume 776, 139008. https://doi.org/10.1016/j.msea.2020.139008
7. Singh, M.P., Shukla, D.K., Kumar, R. and Arora, K.S. (2021), «The structural integrity of high-strength welded pipeline steels: a review», International Journal of Structural Integrity, Vol. 12 No. 3, pp. 470-496. https://doi.org/10.1108/IJSI-05-2020-0051
8. Constant, A., Grumbach, M., Blood, G. (1970). Study of the transformation of the austenite and changes the properties of steels at dispersoids. Metallurgy Review.
9. CSM. (1971). Study of the influence of niobium. ECSC information days Luxembourg.
10. Gladman T. (1966). Proceedings of the Royal Society.
11. Ling, Z.Q., Fang, J., Zhou, Y., Yuan, Z.X. (2012). Influence of quenching on-line on properties of X70 steel for sour service seamless pipe. Energy Procedia, 16, 444-450. https://doi.org/10.1016/j.egypro.2012.01.072
12. Zhao, Am., Wang, Y., Chen, Yl. et al. (2011). Precipitation behaviors of X80 acicular ferrite pipeline steel. Int J Miner Metall Mater 18, 309–313. https://doi.org/10.1007/s12613-011-0439-4
13. Bridge, G., Maynier, P., Dollet, J., Bastien, P. (1970). Contribution to the study of the influence of molybdenum on the softening of activation energy income. Metallurgical News.
14. Lewellym, D.T., Cook, W.T. (1974). Metallurgy of boron tread low-alloy steel. Metals Technology, 1(1): 517-529. https://doi.org/10.1179/030716974803287924
15. G. MURRY. Transformations dans les aciers. Technique de l'ingénieur. Fasc M1115. https://www.techniques-ingenieur.fr/base-documentaire/archives-th12/archives-traitement-des-metaux-tiamd/archive-1/transformations-dans-les-aciers-m1115/#presentation